Mineralogical Magazine, December 2018, Vol. 82(6), pp. 1307–1322

Graftonite-(Mn), ideally $^{M1}\mathrm{Mn}^{M2,M3}\mathrm{Fe}_2(\mathrm{PO}_4)_2$, and graftonite-(Ca), ideally $^{M1}\mathrm{Ca}^{M2,M3}\mathrm{Fe}_2(\mathrm{PO}_4)_2$, two new minerals of the graftonite group from Poland

ADAM PIECZKA[1,*], FRANK C. HAWTHORNE[2], NEIL BALL[2], YASSIR ABDU[2,3], BOŻENA GOŁĘBIOWSKA[1], ADAM WŁODEK[1] AND JAN ŻUKROWSKI[4]

[1] AGH University of Science and Technology, Department of Mineralogy, Petrography and Geochemistry, 30-059 Kraków, Mickiewicza 30, Poland
[2] Department of Geological Sciences, University of Manitoba, Winnipeg, Manitoba R3T 2N2, Canada
[3] Department of Applied Physics and Astronomy, University of Sharjah, P.O. Box 27272, Sharjah, United Arab Emirates
[4] AGH University of Science and Technology, Academic Center for Materials and Nanotechnology, 30-059 Kraków, Mickiewicza 30, Poland

[*Received 30 October 2017; Accepted 31 December 2017; Associate Editor: Giancarlo Della Ventura*]

Abstract

Two new minerals of the graftonite group, graftonite-(Mn), ideally $^{M(1)}\mathrm{Mn}^{M(2),M(3)}\mathrm{Fe}_2(\mathrm{PO}_4)_2$, and graftonite-(Ca), ideally $^{M(1)}\mathrm{Ca}^{M(2),M(3)}\mathrm{Fe}_2(\mathrm{PO}_4)_2$, were discovered in phosphate nodules of two beryl–columbite–phosphate pegmatites at Lutomia and Michałkowa, respectively, in the Góry Sowie Block, Lower Silesia, southwest Poland. Graftonite-(Mn) is pinkish brown, whereas graftonite-(Ca) shows more brownish colouration. Both minerals have a vitreous lustre, a good cleavage observed along (010) and irregular fracture; both are transparent and neither of them is fluorescent. They are brittle and have a Mohs hardness of ~5. The minerals are non-pleochroic, colourless in all orientations, biaxial (+), with mean refractive indices $\alpha = 1.710(2)$ and $1.690(2)$, $\beta = 1.713(2)$ and $1.692(2)$, and $\gamma = 1.725(2)$ and $1.710(5)$, respectively. With complete order of Ca at the $M(1)$ site, the formulae of the holotype crystals are $^{M(1)}(\mathrm{Mn}_{0.70}\mathrm{Ca}_{0.30})^{M(2),M(3)}(\mathrm{Fe}_{1.34}\mathrm{Mn}_{0.60}\mathrm{Mg}_{0.06}\mathrm{Zn}_{0.01})_{\Sigma 3}(\mathrm{PO}_4)_2$ for graftonite-(Mn) and $^{M(1)}(\mathrm{Ca}_{0.98}\mathrm{Mn}_{0.02})^{M(2),M(3)}(\mathrm{Fe}_{1.38}\mathrm{Mn}_{0.56}\ \mathrm{Mg}_{0.05})_{\Sigma 3}(\mathrm{PO}_4)_2$ for graftonite-(Ca). Both crystal chemistry and crystal-structure refinement ($R_1 = 2.34$ and 1.63%, respectively) indicate that the $M(1)$ site is occupied dominantly by Mn in graftonite-(Mn) and by Ca in graftonite-(Ca), and the $M(2)$ and $M(3)$ sites are occupied by Fe^{2+} and Mn^{2+}, with Fe^{2+} dominant over Mn^{2+} at the aggregate $M(2) + M(3)$ sites. Graftonite-(Mn) and graftonite-(Ca) are isostructural with graftonite, $^{M(1)}\mathrm{Fe}^{M(2),M(3)}\mathrm{Fe}_2(\mathrm{PO}_4)_2$ (monoclinic system; space-group symmetry $P2_1/c$), with the unit-cell parameters $a = 8.811(2)$ Å, $b = 11.494(2)$ Å, $c = 6.138(1)$ Å, $\beta = 99.23(3)°$ and $V = 613.5(4)$ Å^3, and $a = 8.792(2)$ Å, $b = 11.743(2)$ Å, $c = 6.169(1)$ Å, $\beta = 99.35(3)°$ and $V = 628.5(1)$ Å^3, respectively. The densities calculated on the basis of molar weights and unit-cell volumes are 3.793 g/cm^3 for graftonite-(Mn) and 3.592 g/cm^3 for graftonite-(Ca). The eight strongest lines in powder X-ray diffraction patterns on the basis of single-crystal data are, respectively [d, Å, I (hkl)]: 2.874, 100, (230 + 040); 2.858, 79, (221); 3.506, 73, (130); 2.717, 79, ($\bar{3}11$); 2.952, 55, (131); 2.916, 53, ($\bar{1}12$); 2.899, 44, (300); 3.016, 35, ($\bar{1}02$); and 3.654, 100, (130); 2.979, 85, (221); 3.014, 77, (230); 3.042, 76, (040 + $\bar{1}12$); 2.834, 68, ($\bar{3}11$); 3.097, 57, (131); 3.133, 56, ($\bar{1}02$); 2.542, 30, (311). Both minerals are common primary phosphates in phosphate nodules, occurring as lamellar intergrowths with sarcopside ± triphylite/

---

*E-mail: pieczka@agh.edu.pl

https://doi.org/10.1180/minmag.2017.081.109

lithiophilite, products of exsolution from a (Li,Ca)-rich graftonite-like parent phase crystallized at high temperature from P-bearing hydrosaline melts.

KEYWORDS: graftonite-(Mn), graftonite-(Ca), Góry Sowie Block, Poland.

Introduction

GRAFTONITE, ideally $Fe_3(PO_4)_2$, and beusite, ideally $Mn_3(PO_4)_2$, form a continuous solid solution: $(Fe^{2+},Mn^{2+},Ca)_3(PO_4)_2$. In addition to triphylite and sarcopside, minerals of the graftonite–beusite series are major accessory, primary phosphate minerals occurring as intergrowths in characteristic nodules in P-bearing pegmatites, especially of the beryl–columbite–phosphate subtype of the rare-element class (Penfield, 1900; Brooks and Shipway, 1960; Fransolet, 1977; Keller *et al.*, 1977; Černý *et al.*, 1998; Smeds *et al.*, 1998; Guastoni *et al.*, 2007; Škoda *et al.*, 2007; Łodziński and Sitarz, 2009; Vignola *et al.*, 2008, 2011*a*,*b*; Tait *et al.*, 2013; Włodek *et al.*, 2015). Graftonite has also been found in amphibolite-facies metamorphosed iron formations (Stalder and Rozendaal, 2002) and as a constituent of iron meteorites (Olsen and Fredriksson, 1966; Bild, 1974; Chen and Xie, 1996; Floss, 1999; Steele *et al.* 1991, Olsen *et al.* 1999; Sharygin *et al.*, 2016).

Calcium has long been considered as a minor constituent substituting for Fe^{2+} and Mn^{2+} in the graftonite–beusite series. However, structural studies (Wise *et al.*, 1990; Tait *et al.*, 2013) have shown that in the graftonite–beusite structure there is complete order of Ca at the $M(1)$ site, followed firstly by Mn^{2+} and then by Fe^{2+}. Remaining Mn and Fe are disordered over the $M(2)$ and $M(3)$ sites in accord with the scheme $M(3) > M(2)$. These findings have enabled a new classification of the graftonite-group minerals (Hawthorne and Pieczka, 2018), earlier considered as the 'graftonite–beusite series'. The classification was approved by the International Mineralogical Association (IMA) Commission on New Minerals, Nomenclature and Classification (CNMNC), as the IMA-CNMNC nomenclature voting proposal 17-H.

This paper presents new mineral descriptions for graftonite-(Ca) and graftonite-(Mn), two of three new mineral species, distinct in the new classification and approved in July 2017 by the IMA-CNMNC (IMA 2017-048 and 2017-050, respectively). Type samples of the both minerals are from two phosphate-bearing pegmatites in Poland; from Lutomia and Michałkowa villages in the gneissic Góry Sowie block. The names graftonite-(Mn) and graftonite-(Ca) are because the minerals are the ${}^{M(1)}$Mn- and ${}^{M(1)}$Ca analogues of graftonite, ${}^{M(1)}Fe^{M(2),M(3)}Fe_2(PO_4)_2$. The holotype and co-type samples are deposited in the collection of the Mineralogical Museum of University of Wrocław (University of Wrocław, Faculty of Earth Science and Environmental Management, Institute of Geological Sciences, Mineralogical Museum, 50-205 Wrocław, Cybulskiego 30, Poland), with catalogue numbers MMWr IV7927 [graftonite-(Mn) holotype], MMWr IV7928 [graftonite-(Mn) co-type], and MMWr IV7674 [graftonite-(Ca) and maneckiite holotype] (Pieczka *et al.*, 2017*a*). The third new mineral species in the graftonite group, beusite-(Ca), with the holotype coming from Canada, is described in a companion paper (Hawthorne *et al.*, 2018). Neither of these minerals was a valid unnamed mineral (Smith and Nickel, 2007; http://pubsites.uws.edu.au/ima-cnmnc/). Graftonite-(Mn) and graftonite-(Ca) are isostructural with graftonite and beusite, with Mn or Ca completely ordered at the $M(1)$ site. In the classification of Strunz (Strunz and Nickel, 2001), it is a class 8.A Phosphate without additional anions, without H_2O. In the classification of Dana (Gaines *et al.*, 1997), it is a class 38 Anhydrous normal phosphate isostructural with graftonite (38.3.3.1) and beusite (38.3.3.2).

Geological setting

Graftonite-(Mn) and graftonite-(Ca) were collected in two phosphate-bearing pegmatites exposed in the Góry Sowie gneissic block, one of the main tectono-stratigraphic units (~650 km^2) of the Sudetes, southwest Poland (northeast part of the Bohemian massif) (Fig. 1). The Góry Sowie gneissic block consists mainly of gneisses and migmatites with minor amphibolites, and is considered to be a fragment of the lower crust (for details see Mazur *et al.*, 2006). The unit is a product of multistage evolution that culminated ~385–370 Ma in amphibolite-facies metamorphism and migmatization at temperatures of 775–910°C and pressures of 6.5–8.5 kbar, and was followed by rapid uplift and exhumation

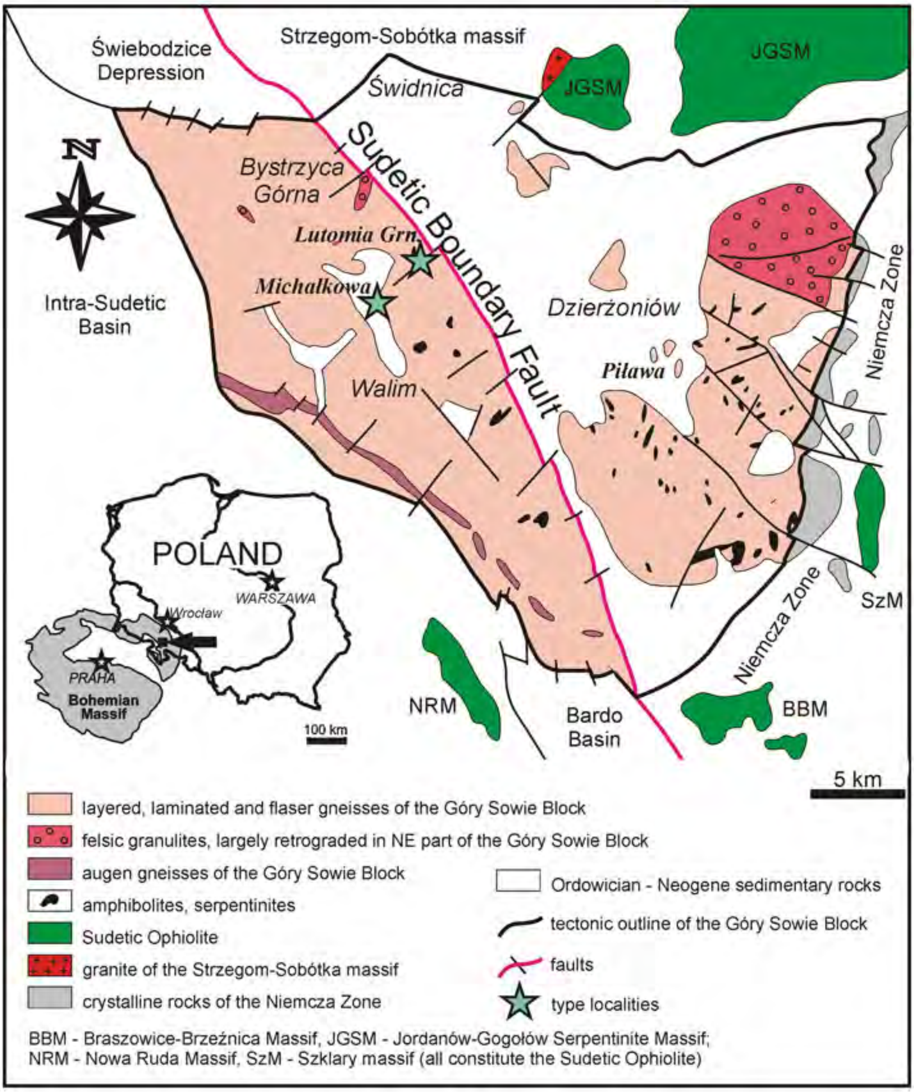

FIG. 1. Geological map of the Góry Sowie Block (after Szuszkiewicz *et al*., 2013) with localities of the Lutomia and Michałkowa pegmatites marked with green stars.

(Brueckner *et al*., 1996; O'Brien *et al*., 1997; Kryza and Fanning, 2007). Anatectic melts, generated by partial melting of the metasedimentary–metavolcanic sequence, were injected as pegmatites and granite-like bodies during decompression, forming small concordant segregations and N-trending discordant dykes in migmatized gneisses and amphibolites (Kryza, 1981; van Breemen *et al*., 1988; Żelaźniewicz, 1990; Bröcker *et al*., 1998; Timmermann *et al*., 2000; Aftalion and Bowes, 2002; Gordon *et al*., 2005). The latter sometimes form large systems of barren to rare-element pegmatites of different affiliations [NYF (niobium-yttrium-fluorine), LCT (lithium-caesium-tantalum) to mixed NYF + LCT], e.g. the Julianna system at Piława Górna (Pieczka *et al*., 2013, 2014, 2015*a*,*b*, 2016, 2017*b*; Szuszkiewicz *et al*., 2013, 2016; Szełęg *et al*., 2017).

Graftonite-(Mn) was found in a pegmatite cropping out in a small abandoned quarry at

Lutomia (50°45′N, 16°29′E), a village ~5 km southeast of Świdnica and ~60 km southwest of Wrocław. The pegmatite forms a relatively large, discordant vertical vein, ~20 m long and up to 1 m thick, hosted by migmatite and amphibolite, with local swellings up to 2 m across, and a few smaller offshoots. The pegmatite is of the beryl–columbite–phosphate subtype of rare-element pegmatites *sensu* Černý and Ercit (2005) or phosphate subtype of rare-element pegmatites *sensu* Novák (2005). It shows, especially in the swellings, well-developed although not continuous zonation (wall zone – graphic zone – blocky feldspars zone – massive albite). The border and wall zones are composed of fine- to medium-grained plagioclase + quartz + 'biotite' (altered) ± K-feldspars ± apatite group ± almandine graphic zone of intergrowths of plagioclase + K-feldspar + quartz ± 'biotite'/muscovite ± tourmaline ± phosphates (rare); blocky feldspar zone of coarse-grained K-feldspar + plagioclase + quartz ± 'biotite'/muscovite + tourmaline + phosphates (rare nodules); and massive albite with rare phosphate nodules disseminated locally. No quartz core is observed. Beside the aforementioned rock-forming minerals, phosphate nodules, reaching to 5 cm × 3 cm × 3 cm in size, contain a large number of phosphate minerals, e.g. monazite-(Ce), xenotime-(Y), graftonite-(Mn), graftonite-(Ca), beusite-(Ca), sarcopside, triphylite partly oxidized topotactically to ferrisicklerite and heterosite, wolfeite, triploidite, staněkite, hagendorfite, ferrohagendorfite, alluaudite, fluorapatite and hydroxylapatite, whitlockite, kryzhanovskite, phosphoferrite, ludlamite, vivianite, fairfieldite, hureaulite, earlshannonite, whitmoreite, strunzite, ferrostrunzite, beraunite, dufrénite, landesite, jahnsite-(CaMnFe), -(CaMnMn) and -(MnMnMn), and occasionally also malhmoodite and zigrasite (Pieczka *et al.*, 2003; Włodek *et al.*, 2015; Włodek and Pieczka, 2017). The following minerals were found as tiny inclusions in the phosphates or in the rock-forming minerals: fergusonite-(Y), gadolinite-(Y), allanite-(Ce), ilmenite, titanite, sillimanite ('fibrolite'), uraninite, pyrite, arsenopyrite, löllingite, chalcopyrite, Cd-bearing wurtzite or sphalerite, chalcocite or covellite, cuprite, native copper, goethite and unidentified Mn oxides (Pieczka *et al.*, 2015*c*; Włodek *et al.*, 2015).

Graftonite-(Ca) was collected at Michałkowa (50°45′N, 16°27′E), in the middle part of the Góry Sowie Block, ~70 km southwest of Wrocław, on a small pegmatite dump, a relic of excavation in the ninteenth century as a source of quartz and feldspar. During this work, Websky (1868) found and described sarcopside (type locality), associated with hureaulite, vivianite and an apatite-group mineral. The dump is located on the left site of the Dział Michałowski Range, on the right side of the Młynówka stream, ~100 m from the Zagórze Śląskie – Lubachów – Michałkowa – Pieszyce road. The original pegmatite vein, ~10–12 m long and 2–4 m thick, with visible zoning (wall zone – graphic zone – blocky feldspar zone), was composed of albite, microcline, quartz, muscovite, 'biotite', schorl evolving to foitite, almandine, sillimanite, andalusite and phosphate minerals in nodules reaching a few centimetres in diameter (Łodziński and Sitarz, 2009). Graftonite-(Ca) was found in an outer zone of a small phosphate nodule (~2 cm in diameter) collected on the dump. The nodule was composed mainly of lamellar intergrowths of the primary magmatic phosphates: sarcopside and graftonite-(Mn), with minor triphylite oxidized topotactically to ferrisicklerite and heterosite. In this zone, the magmatic phosphates underwent intensive Na and Ca metasomatism and were replaced by wolfeite, alluaudite, maneckiite, fluorapatite and hydroxylapatite, in places forming fine-grained mosaics (Pieczka *et al.*, 2017*a*). To date, ~50 phosphate minerals have been identified in the pegmatite (Grochowina, 2016), including rare species such as maneckiite (type locality), wicksite, wyllieite, ferrowyllieite, qingheiite-(Fe), maghagendorfite, hagendorfite, ferrohagendorfite, johnsomervilleite, lazulite, gormanite, childrenite, souzalite and arrojadite-(KNa). Łodziński and Sitarz (2009) also mentioned the presence of qingheiite, rosemaryite and simferite in nodules of the pegmatite, but these phosphates have not yet been confirmed by chemical analysis or X-ray diffraction.

Physical and optical properties

Graftonite-(Mn) occurs in the Lutomia pegmatite as lamellar intergrowths with triphylite or products of its topotactic oxidation: ferrisicklerite and heterosite, in the form of pinkish-brown lamellae up to 0.5 mm wide. Along fissures, the mineral and associated triphylite were Na- and Ca-metasomatized, commonly forming symplectic intergrowths of alluaudite-group minerals with wolfeite and staněkite, and sometimes with whitlockite. Sarcopside, up to 50 μm thick and several hundred μm long, as one or two independent sets of diagonally arranged and criss-crossing needles, occurs only locally as inclusions in triphylite and products of its topotactic oxidation. No direct intergrowths of graftonite-(Mn) with sarcopside were observed (Włodek *et al*., 2015). Towards the border of the nodule, the amount of graftonite-(Mn)–triphylite intergrowths generally decreases, and graftonite-(Mn) may occur in massive accumulations (Fig. 2a,*b*).

In the Michałkowa pegmatite, graftonite-(Mn) commonly evolves towards graftonite-(Ca). Graftonite with very high Ca content, close in composition to end-member graftonite-(Ca) is less common. One such crystal, ~70 µm × 100 µm, was found as an intergrowth with maneckiite, close to the border of the metasomatic phosphates with the primary magmatic phosphates of the unaltered interior of the nodule (Pieczka *et al*., 2015*a*), overgrown by a mosaic of wolfeite, alluaudite and hydroxylapatite (Fig. 2c,*d*).

Graftonite-(Mn) is pinkish brown, whereas graftonite-(Ca) shows rather more brownish colouration. Both minerals have a colourless streak and vitreous lustre and are transparent. Neither of them is fluorescent. Both minerals have good cleavage along (010), irregular fracture and no observed parting. They are brittle and have a Mohs hardness of ~5 by analogy with graftonite. The densities, calculated on the basis of molar weights and unit-cell volumes, are 3.793 g/cm^3 for the refined crystal of graftonite-(Mn) and 3.592 g/cm^3 for graftonite-(Ca). Both minerals are non-pleochroic, colourless in all orientations, biaxial (+), with mean refractive indices $\alpha = 1.710(2)$ and $1.690(2)$, $\beta = 1.713(2)$ and $1.692(2)$, and $\gamma = 1.725(2)$ and $1.710(5)$,

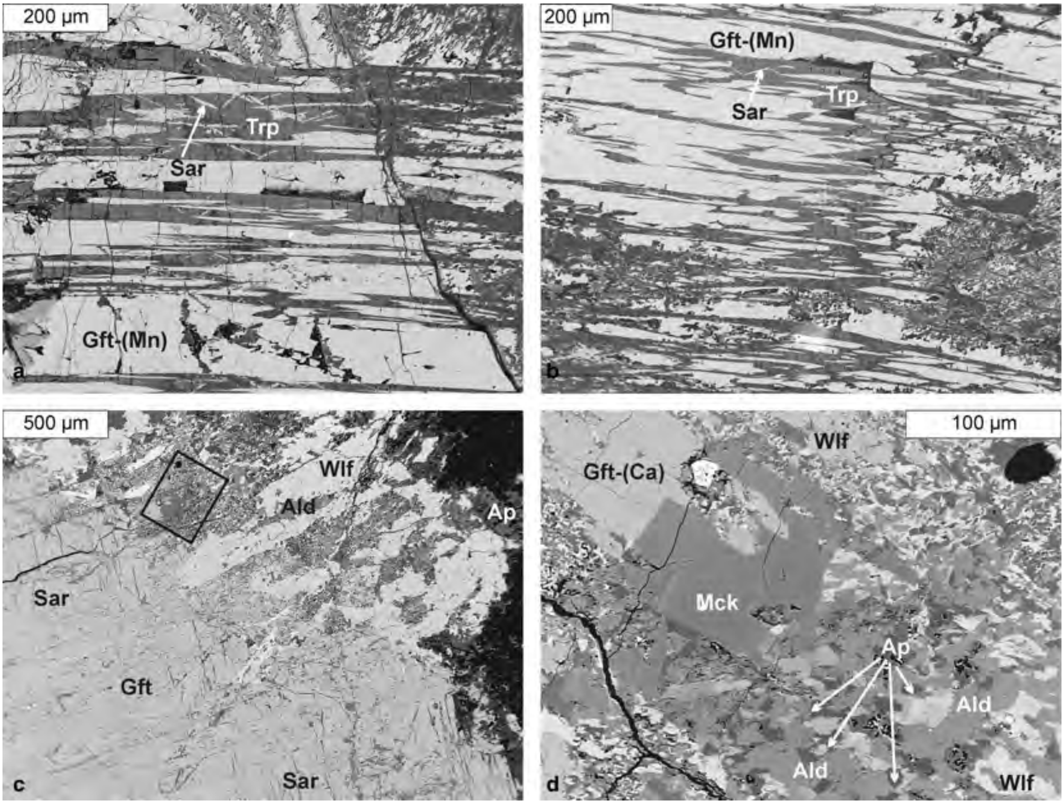

FIG. 2. Back-scatter electron images. (*a*, *b*) Lamellar intergrowths of graftonite-(Mn) with triphylite (ferrisicklerite/heterosite) in the Lutomia pegmatite; (*c*) a fragment of a phosphate nodule from Michałkowa with graftonite-(Ca) (framed, *d*) intergrown with maneckiite in a mosaic of metasomatic alluaudite, wolfeite and hydroxylapaite. Abbreviations: Ald = alluaudite-group minerals, Ap = hydroxylapatite, Gft-(Ca) = graftonite-(Ca), Gft-(Mn) = graftonite-(Mn), Mck = maneckiite, Sar = sarcopside, Trp = triphylite and Wlf = wolfeite.

respectively, and $2V_{\text{meas.}} = 54(2)°$ and $40.1(6)°$ and $2V_{\text{calc.}} = 53.4°$ and $37\ °$ (wavelength 589 nm). The optical orientations are: $X \parallel \mathbf{b}$, $Y \wedge \mathbf{a} = 44.2°$ (in β obtuse), $Z \wedge \mathbf{c} = 35.0°$ (in β acute) for graftonite-(Mn), and $X \parallel \mathbf{b}$, $Y \wedge \mathbf{a} = 41.4°$ in β acute and $Z \wedge \mathbf{c} = 32.1°$ in β acute for graftonite-(Ca).

Chemical composition

Electron-microprobe analysis was undertaken at the Inter-Institute Analytical Complex for Minerals and Synthetic Substances at the University of Warsaw, using a Cameca SX 100 electron microprobe operating in wavelength-dispersive mode under the following conditions: accelerating voltage of 15 kV, beam current of 20 nA, beam diameter of 2 µm, peak count-time of 20 s, background time of 10 s. Standards (element, analytical lines, diffracting crystals and mean detection limits in wt.%) were as follows: YP_5O_{14} (P*K*α, PET, 0.02); diopside (Mg*K*α, TAP, 0.01) and (Ca*K*α, PET, 0.02); rhodonite (Mn*K*α, LIF, 0.06); hematite (Fe*K*α, LIF, 0.06); and sphalerite (Zn*K*α, LIF, 0.06). The raw data were reduced with the 'PAP' routine of Pouchou and Pichoir (1985). The formulae were normalized to 8 O atoms per formula unit (apfu).

Chemical compositions are presented in Table 1. Average compositions of the holotype crystals correspond to following formulae: $(Fe_{1.34}Mn_{1.30}Ca_{0.30}Mg_{0.06}Zn_{0.01})_{\Sigma 3.00}(PO_4)_{1.99}$ and $(Fe_{1.38}Ca_{0.98}Mn_{0.58}Mg_{0.05})_{\Sigma 2.99}(PO_4)_{2.00}$. Assuming complete order of Ca at the *M*(1) site and omitting minor inaccuracies in the contents of cations and PO_4 anion, the optimized formulae are $^{M(1)}(Mn_{0.70}Ca_{0.30})^{M(2),M(3)}(Fe_{1.34}Mn_{0.60}Mg_{0.06}Zn_{0.01})_{\Sigma 3}(PO_4)_2$ and $^{M(1)}(Ca_{0.98}Mn_{0.02})^{M(2),M(3)}(Fe_{1.38}Mn_{0.56}Mg_{0.05})_{\Sigma 3}(PO_4)_2$ for the holotype samples. The compositions indicate that the *M*(1) site should be dominated by Mn^{2+} in graftonite-(Mn) and by Ca^{2+} in graftonite-(Ca). In both minerals, the $M(2) + M(3)$ sites are dominated by Fe^{2+}, with a probable tendency to partial order of Mn^{2+} at the *M*(3) site and dominance of Fe^{2+} at the *M*(2) site.

Raman spectroscopy

The Raman spectrum of graftonite-(Mn) was collected in back-scattered mode at the Faculty of Materials Science and Ceramics, AGH UST, Kraków, Poland, with a Horiba Labram HR spectrometer integrated with an Olympus BX 40 confocal microscope, equipped with a 532 nm Nd:YAG laser, (10 mW), grating 1800 gr/mm. The

TABLE 1. Chemical compositions of graftonite-(Mn) and graftonite-(Ca)*.

	Graftonite-(Mn)				Graftonite-(Ca)			
Constituent	wt.%	range	S.D.	Ideal wt.%	wt.%	range	S.D.	Ideal wt.%
P_2O_5	40.02	39.62–40.46	0.23	39.81	41.52	41.36–41.68	0.22	41.54
FeO	27.31	26.07–28.83	0.81	40.03	29.13	27.81–30.44	1.86	42.05
MnO	26.06	25.61–26.46	0.30	19.89	12.14	11.34–12.94	1.13	
MgO	0.66	0.57–0.74	0.05		0.56	0.09–1.03	0.66	
CaO	4.74	3.74–5.97	0.76		16.17	16.05–16.28	0.16	16.41
ZnO	0.29	0.20–0.36	0.05		b.d.l.	b.d.l.		
Total	99.09	98.48–99.92	0.40	100.00	99.51	99.28–99.73	0.32	100.00
Atoms per formula unit on the basis of 8 O								
PO_4^{3-}	1.99	1.99–2.00	<0.01	2	2.00	2.00	<0.01	2
Fe^{2+}	1.34	1.29–1.41	0.04	2	1.39	1.32–1.46	0.10	2
Mn^{2+}	1.30	1.27–1.33	0.02	1	0.58	0.55–0.62	0.05	
Mg^{2+}	0.05	0.05–0.06	<0.01		0.05	0.01–0.09	0.06	
Ca^{2+}	0.30	0.24–0.38	0.05		0.98	0.98–0.99	<0.01	1
Zn^{2+}	0.01	0.01–0.02	<0.01		0.00	0.00		
Mn/(Mn + Fe)	0.49	0.48–0.50	0.01		0.30	0.27–0.32	0.03	

*Number of analytical spots = 20 for graftonite-(Mn) and 2 for graftonite-(Ca).
b.d.l. = below detection limit; S.D. = standard deviation.

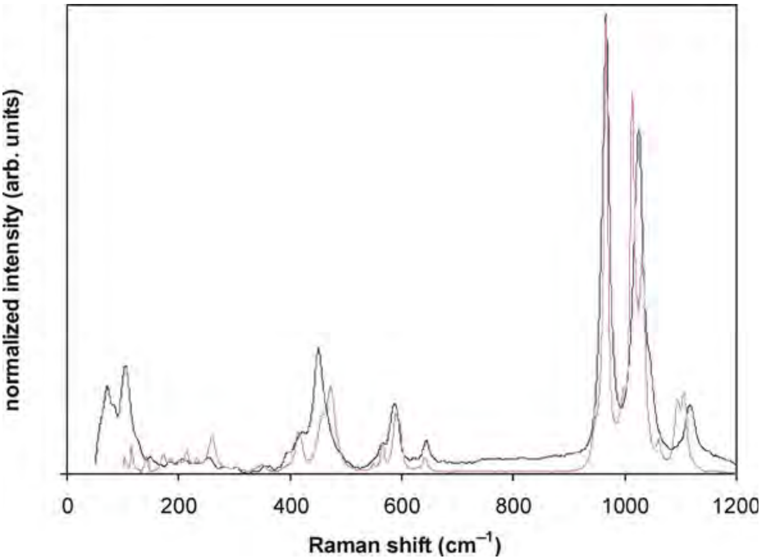

FIG. 3. Raman spectra of graftonite-(Mn) (black) and graftonite-(Ca) (violet).

spectrum was recorded in the range 4000–50 cm^{-1} at a magnification of 100×, with resolution of 0.5 cm^{-1}, an acquisition time of 600 s, and accumulation of 2 scans with an estimated spot size ~1 μm. The spectrum of graftonite-(Ca) was collected in back-scattered mode at the Department of Geological Sciences, University of Manitoba, Winnipeg, Canada, with a Horiba Jobin Yvon-LabRAM ARAMIS integrated confocal micro-Raman system equipped with a 460 mm focal length spectrograph and a multichannel air-cooled (–70°C) CCD detector. A magnification of 100×

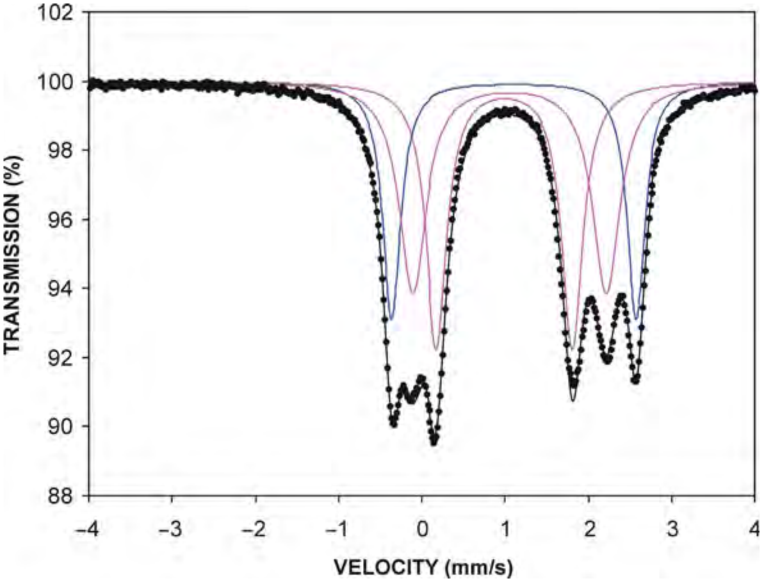

FIG. 4. Mössbauer spectrum of graftonite-(Mn); quadrupole-doublets are marked in violet. The quadrupole-doublet in blue originates from intergrown triphylite.

TABLE 2. Resolution of Mössbauer spectrum of graftonite-(Mn).

IS (mm/s)	QS (mm/s)	Γ/2 (mm/s)	Rel. Int. (%)	Comments
1.2155	2.934(2)	0.128(1)	27.08	Triphylite
1.1619	2.327(3)	0.198(3)	37.02 (50.77*)	Graftonite-(Mn)
0.9938	1.636(2)	0.152(1)	35.90 (49.23*)	Graftonite-(Mn)

IS – isomeric shift; QS – quadropole splitting; Γ = half of width at half of maximum.
*Data recalculated to 100%.

was used with an estimated spot size of 1 μm, a 1800 gr/mm grating, an excitation radiation of 532 nm, and a laser power between 5 and 12.5 mW. Calibration in both laboratories was done using the 520.7 cm^{-1} line of Si. The spectra are presented in Fig. 3.

The peaks at ~966 (strong), 1025 (medium) and 1117 (weak) cm^{-1} in the Raman spectrum of graftonite-(Mn), and ~968, 1013 and 1032 cm^{-1} (strong) and 1098 and 1106 cm^{-1} (medium) in the spectrum of graftonite-(Ca) may be assigned to stretching vibrations of the PO_4 groups. The peaks at 587, 566, 451 and 423 cm^{-1} [graftonite-(Mn)] and at 590, 472 and 458 cm^{-1} [graftonite-(Ca)] are due to the bending vibrations of PO_4. The weaker peaks below ~400 cm^{-1} are due to deformations of the Ca and Mn polyhedra.

Mössbauer spectroscopy

The ^{57}Fe Mössbauer absorption spectrum of graftonite-(Mn) (Fig. 4) was collected at room temperature, at the Academic Center for Materials and Nanotechnology, AGH UST, Kraków, Poland, using a ^{57}Co source in the Rh matrix. A Mössbauer spectrometer of an electromechanical type was used

TABLE 3. Miscellaneous information for graftonite-(Mn) and graftonite-(Ca).

	Graftonite-(Mn)	Graftonite-(Ca)
Crystal data		
Crystal size (μm)	40 × 80 × 120	35 × 40 × 45
Space group	$P2_1/c$	$P2_1/c$
a (Å)	8.811(2)	8.792(2)
b	11.494(2)	11.743(2)
c	6.138(1)	6.169(1)
β (°)	99.23(3)	99.35(3)
V (Å^3)	613.5(4)	628.5(4)
Z	4	4
a:b:c	0.7666:1:0.5341	0.7887:1:0.5253
Data collection		
Radiation	Mo$K\alpha$	Mo$K\alpha$
No. of reflections	7808	7385
No. unique reflections	1961	1856
No. with ($F_o > 4\sigma F$)	1911	1793
Structure refinement		
R_{int}%	1.31	1.45
R_1%	2.34	1.63
wR_2%	6.69	4.56

$R_1 = \Sigma(|F_o| - |F_c|)/\Sigma|F_o|$; $wR_2 = [\Sigma w(F_o^2 - F_c^2)^2/\Sigma w(F_o^2)^2]^{½}$, $w = 1/[\sigma^2(F_o^2) + (0.0288P)^2 + 0.79P]$ where $P = (\mathrm{Max}(F_o^2,0) + 2F_c^2)$.

TABLE 4. Atom coordinates and displacement parameters for graftonite-(Mn).

Atom	x	y	z	U^{11}	U^{22}	U^{33}	U^{23}	U^{13}	U^{12}	U_{eq}
M(1)	0.94506(4)	0.11902(3)	0.84012(6)	0.02026(19)	0.01344(17)	0.02277(19)	−0.00414(12)	−0.00343(13)	0.00131(12)	0.01958(12)
M(3)	0.71753(4)	0.07905(4)	0.32823(5)	0.02119(19)	0.0343(2)	0.00704(16)	0.00013(12)	0.00217(11)	0.00886(14)	0.02086(12)
M(3)	0.36281(4)	0.19156(3)	0.12765(5)	0.01398(16)	0.01189(15)	0.01003(15)	0.00016(9)	0.00129(10)	0.00197(10)	0.01203(10)
P(1)	0.09333(5)	0.13552(4)	0.39525(8)	0.0086(2)	0.0100(2)	0.0085(2)	−0.00067(15)	0.00188(15)	−0.00107(15)	0.00896(12)
P(2)	0.60376(6)	0.08846(4)	0.80663(8)	0.0086(2)	0.0102(2)	0.0064(2)	0.00013(14)	0.00171(15)	0.00102(15)	0.00837(12)
O(1)	0.07757(19)	0.06816(14)	0.1771(3)	0.0186(7)	0.0134(6)	0.0110(6)	−0.0033(5)	0.0024(5)	0.0007(5)	0.0143(3)
O(2)	0.47686(18)	0.17678(13)	0.8298(3)	0.0130(6)	0.0149(7)	0.0125(6)	0.0017(5)	0.0031(5)	0.0054(5)	0.0133(3)
O(3)	0.9419(2)	0.19814(16)	0.4162(3)	0.0138(7)	0.0300(9)	0.0223(8)	−0.0072(7)	0.0059(6)	0.0058(6)	0.0217(4)
O(4)	0.69379(18)	0.12658(13)	0.6248(2)	0.0144(7)	0.0171(7)	0.0085(6)	0.0008(5)	0.0049(5)	−0.0018(5)	0.0130(3)
O(5)	0.2190(2)	0.22755(15)	0.3812(3)	0.0221(8)	0.0202(7)	0.0125(6)	−0.0008(6)	0.0046(6)	−0.0130(6)	0.0181(3)
O(6)	0.72647(17)	0.08814(14)	0.0152(2)	0.0102(6)	0.0200(7)	0.0073(6)	−0.0002(5)	0.0001(5)	0.0016(5)	0.0126(3)
O(7)	0.1370(2)	0.06060(14)	0.5999(3)	0.0275(9)	0.0142(7)	0.0129(7)	0.0051(5)	−0.0024(6)	−0.0049(6)	0.0188(3)
O(8)	0.53395(17)	−0.03486(13)	0.7619(2)	0.0121(6)	0.0107(6)	0.0129(6)	0.0000(5)	0.0013(5)	−0.0011(5)	0.0120(3)

TABLE 5. Atom coordinates and displacement parameters for graftonite-(Ca).

Atom	x	y	z	U^{11}	U^{22}	U^{33}	U^{23}	U^{13}	U^{12}	U_{eq}
M(1)	0.95075(3)	0.12407(2)	0.82659(5)	0.01412(15)	0.01124(14)	0.01052(14)	−0.00061(9)	0.00090(10)	−0.00024(9)	0.01208(9)
M(2)	0.71201(3)	0.08002(2)	0.32618(3)	0.01432(12)	0.01943(13)	0.00583(11)	0.00027(7)	0.00135(8)	0.00428(8)	0.01323(8)
M(3)	0.35994(3)	0.19058(2)	0.13322(4)	0.01407(12)	0.01357(12)	0.00900(12)	0.00021(7)	0.00107(8)	0.00247(8)	0.01230(8)
P(1)	0.09429(4)	0.13313(3)	0.39783(6)	0.00918(16)	0.00907(16)	0.00734(16)	0.00003(11)	0.00160(12)	−0.00047(11)	0.00850(9)
P(2)	0.59969(4)	0.08932(3)	0.80729(6)	0.00871(16)	0.01132(17)	0.00563(15)	−0.00008(11)	0.00144(12)	0.00045(12)	0.00852(9)
O(1)	0.08319(14)	0.07107(9)	0.17821(18)	0.0184(5)	0.0120(5)	0.0084(5)	−0.0021(4)	0.0019(4)	0.0013(4)	0.0130(2)
O(2)	0.47048(13)	0.17453(10)	0.83106(18)	0.0121(5)	0.0166(5)	0.0106(5)	0.0013(4)	0.0033(4)	0.0051(4)	0.0129(2)
O(3)	0.93834(13)	0.18602(9)	0.42934(19)	0.0118(5)	0.0141(5)	0.0125(5)	0.0009(4)	0.0039(4)	0.0029(4)	0.0126(2)
O(4)	0.68469(12)	0.12779(10)	0.62166(17)	0.0133(5)	0.0159(5)	0.0069(4)	−0.0001(4)	0.0032(4)	−0.0014(4)	0.0119(2)
O(5)	0.20933(13)	0.23233(10)	0.38521(18)	0.0167(5)	0.0161(5)	0.0108(5)	−0.0008(4)	0.0035(4)	−0.0077(4)	0.0144(2)
O(6)	0.72450(13)	0.09199(10)	0.01348(17)	0.0108(5)	0.0192(5)	0.0057(4)	0.0003(4)	0.0004(4)	−0.0001(4)	0.0120(2)
O(7)	0.14641(13)	0.05815(10)	0.59776(18)	0.0149(5)	0.0127(5)	0.0098(5)	0.0026(4)	0.0007(4)	0.0014(4)	0.0126(2)
O(8)	0.53474(12)	−0.03324(9)	0.76596(18)	0.0120(5)	0.0118(5)	0.0120(5)	−0.0007(4)	0.0015(4)	−0.0019(4)	0.0120(2)

in the constant-acceleration mode. The 14.4 keV γ-rays were detected with a proportional counter. The velocity scale was calibrated at room temperature with a metallic iron foil. The spectrum was analysed by least-squares fitting, assuming three quadrupole-split spectrum components, corresponding to different Fe positions (Table 2).

The outer doublet in the spectrum, with relative intensity 27.08% is due to triphylite. Two inner doublets, with comparable relative intensities of 50.8 and 49.2% (total recalculated to 100 relative %), are due to graftonite-(Mn). They indicate that in the Lutomia graftonite-(Mn), Fe is completely disordered over the *M*(2) and *M*(3) sites, which leads to the structural formula $^{M(1)}(\mathrm{Mn}_{0.70}\mathrm{Ca}_{0.30})^{M(2)}(\mathrm{Fe}_{0.67}\mathrm{Mn}_{0.27}\mathrm{Mg}_{0.06}\mathrm{Zn}_{0.01})^{M(3)}(\mathrm{Fe}_{0.67}\mathrm{Mn}_{0.33})_{\Sigma3.00}(\mathrm{PO}_4)_2$, corresponding to the general formula $\mathrm{MnFe}_2(\mathrm{PO}_4)_2$ for the graftonite-(Mn) end-member.

TABLE 6. Interatomic distances (Å) in graftonite-(Mn) and graftonite-(Ca).

	Graftonite–(Mn)	Graftonite–(Ca)
M(1)–O(1A)	2.162(2)	2.310(1)
M(1)–O(1B)	2.282(2)	2.372(1)
M(1)–O(3)	2.752(2)	2.542(1)
M(1)–O(3B)	2.154(2)	2.326(1)
M(1)–O(4)	2.391(2)	2.472(1)
M(1)–O(5)	2.967(2)	2.807(1)
M(1)–O(6)	2.378(2)	2.485(1)
M(1)–O(7)	2.507(2)	2.518(1)
<*M*(1)–O>	2.449	2.479
M(2)–O(3)	2.394(2)	2.346(1)
M(2)–O(4)	1.944(2)	1.959(1)
M(2)–O(6)	1.938(2)	1.955(1)
M(2)–O(7)	2.057(2)	2.052(1)
M(2)–O(8)	2.254(2)	2.221(1)
<M(2)–O>	2.117	2.107
M(3)–O(1)	2.943(2)	2.861(1)
M(3)–O(2A)	2.230(2)	2.246(1)
M(3)–O(2B)	2.107(2)	2.135(1)
M(3)–O(5)	2.198(2)	2.254(1)
M(3)–O(5B)	2.036(2)	2.063(1)
M(3)–O(8)	2.082(2)	2.115(1)
<*M*(3)–O>	2.266	2.279
P(1)–O(1)	1.534(2)	1.527(1)
P(1)–O(3)	1.540(2)	1.546(1)
P(1)–O(5)	1.543(2)	1.553(1)
P(1)–O(7)	1.521(2)	1.524(1)
<*P*(1)–O>	1.535	1.538
P(2)–O(2)	1.533(2)	1.539(1)
P(2)–O(4)	1.533(2)	1.534(1)
P(2)–O(6)	1.537(2)	1.539(1)
P(2)–O(8)	1.552(2)	1.554(1)
<*P*(2)–O>	1.539	1.542

Crystal structure

Single crystals of graftonite-(Mn) (40 μm × 80 μm × 120 μm) and graftonite-(Ca) (35 μm × 40 μm × 45 μm) were attached to tapered glass fibres and mounted on a Bruker APEX II ULTRA three-circle diffractometer equipped with a rotating-anode generator (Mo*K*α X-radiation), multilayer optics and an APEX-II detector. For graftonite-(Mn), a total of 7808 intensities was collected to 62° (2θ) using 2 s per 0.3° frame; for graftonite-(Ca), a total of 7385 intensities was collected to 60° (2θ) using 16 s per 0.3° frame, with a crystal-to-detector distance of 5 cm for both crystals. Empirical absorption corrections (*SADABS*; Sheldrick, 2008) were applied and equivalent reflections were merged, resulting in 1961 unique reflections for graftonite-(Mn) and 1856 unique reflections

TABLE 7. Site-scattering values (epfu) and site populations (apfu) in graftonite-(Mn) and graftonite-(Ca).

Site	Site scattering	[CN]	<*M*–O> Å	Site populations	Calculated site-scattering
Graftonite-(Mn)					
M(1)	25.51(7)	[8]	2.449	$0.30\mathrm{Ca} + 0.70\mathrm{Mn}^{2+}$	23.5
M(2)	25.34(7)	[5]	2.117	$0.67\mathrm{Fe}^{2+} + 0.27\mathrm{Mn}^{2+} + 0.06\mathrm{Mg}$	24.9
M(3)	25.39(7)	[6]	2.266	$0.67\mathrm{Fe}^{2+} + 0.33\mathrm{Mn}^{2+}$	25.7
Graftonite-(Ca)					
M(1)	20.80(4)	[8]	2.479	$0.98\mathrm{Ca} + 0.02\mathrm{Mn}^{2+}$	20.1
M(2)	26.01(5)	[5]	2.107	$1.00\mathrm{Fe}^{2+}$	26.0
M(3)	25.44(5)	[6]	2.279	$0.39\mathrm{Fe}^{2+} + 0.56\mathrm{Mn}^{2+} + 0.05\mathrm{Mg}$	24.7

epfu – electrons per formula unit; apfu – atoms per formula unit; [CN] – coordination number.

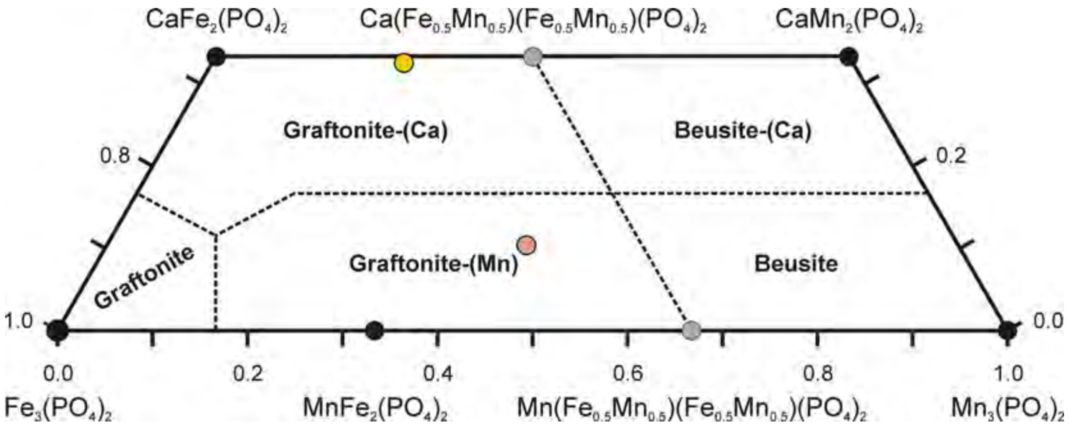

FIG. 5. Compositional plot for the $Fe_3(PO_4)$–$Mn_3(PO_4)$–$CaFe_2(PO_4)$–$CaMn_2(PO_4)$ system with the positions of average compositions of type graftonite-(Mn) and graftonite-(Ca).

for graftonite-(Ca). Unit-cell dimensions were obtained by least-squares refinement of the positions of 4073 reflections with $I > 10\sigma I$ for graftonite-(Mn), and of 9896 reflections for graftonite-(Ca) (Table 3). The structures were refined to R_1 indexes of 2.34% for graftonite-(Mn) and 1.63% for graftonite-(Ca). Atom positions and equivalent isotropic-displacement parameters are given in Tables 4 and 5, respectively, selected interatomic distances in Table 6, and refined site-scattering values (Hawthorne *et al.*, 1995) and assigned site-populations in Table 7. Observed and calculated structure-factors and a crystallographic information file have been deposited with the Principal Editor of *Mineralogical Magazine* and are available as supplementary material (see below).

Graftonite-(Mn) and graftonite-(Ca) are isostructural with graftonite (Calvo, 1968) and beusite (Tait *et al.*, 2013) (monoclinic system; space-group symmetry $P2_1/c$), with refined site-scattering values given in Table 6. These results are compatible with the compositions determined by electron-microprobe analysis, and show that the $M(1)$ site is occupied dominantly by Mn^{2+} in graftonite-(Mn) and by Ca^{2+} in graftonite-(Ca), and the $M(2)$ and $M(3)$ sites are occupied by Fe^{2+} and Mn^{2+}, with Fe^{2+} dominant over Mn^{2+} at the aggregate $M(2) + M(3)$ sites (Fig. 5). The sizes and heterogeneity of the samples did not provide sufficient materials of the composition of graftonite-(Mn) and graftonite-(Ca) to allow collection of powder-diffraction data. Thus, we collapsed the single-crystal data to two-dimensional experimental diffraction patterns that simulate those of powder patterns (in much the same way as a Gandolfi camera). The patterns are shown in Tables 8 and 9.

Origin

Graftonite-(Mn) and graftonite-(Ca) are common products of magmatic crystallization of P-bearing hydrosaline melts in the form of a (Li,Ca)-rich graftonite-like parent phase, after dissolution of a cooling parental P-bearing silicate melt into aluminosilicate and hydrosaline melts connected with separation of a fluid of lower salinity (Simmons and Webber (2008) and discussion therein). This high-temperature graftonite-like phase exsolves during cooling to a member of the graftonite group, sarcopside and triphylite or lithiophylite, occurring commonly as lamellar intergrowths.

At Lutomia in the Góry Sowie gneissic block [type locality for graftonite-(Mn)], lamellar and granular graftonite-(Mn) occurs with triphylite and sarcopside in an anatectic pegmatite of LCT affinity, of ~380 Ma, coeval with the younger stage of Góry Sowie gneissic block metamorphism of 385–370 Ma in age (van Breemen *et al.*, 1988; Timmermann *et al.*, 2000; Turniak *et al.*, 2015). Graftonite-(Mn) evolves toward graftonite-(Ca), rarely reaching compositions with $^{M(1)}Ca > {}^{M(1)}Mn$. Ca-rich graftonite-(Ca) and beusite-(Ca), with Ca, Fe and Mn each close to 1 apfu, occur in the pegmatite only as irregular domains in lamellae of graftonite-(Mn) and occasionally as thin overgrowths on granular graftonite-(Mn) in fissure

TABLE 8. Simulated powder pattern for graftonite-(Mn).

I	*d* (Å)	*h*	*k*	*l*	*I*	*d* (Å)	*h*	*k*	*l*
13	4.298	1	1	1	16	1.963	$\bar{3}$	2	2
12	3.639	$\bar{2}$	1	1	8	1.944	3	0	2
73	3.506	1	3	0	20	1.927	$\bar{2}$	1	3
7	3.164	2	1	1			$\bar{1}$	2	3
35	3.016	$\bar{1}$	0	2	6	1.906	0	2	3
55	2.953	1	3	1	14	1.892	$\bar{4}$	1	2
53	2.916	$\bar{1}$	1	2			4	3	0
44	2.899	3	0	0	11	1.871	3	4	1
100	2.874	2	3	0			1	6	0
		0	4	0	6	1.851	$\bar{2}$	2	3
79	2.858	2	2	1	17	1.827	$\bar{1}$	5	2
10	2.813	3	2	1			0	6	1
56	2.717	$\bar{3}$	1	1	10	1.803	$\bar{1}$	6	1
15	2.680	0	2	2			1	2	3
15	2.655	1	1	2			$\bar{1}$	3	3
7	2.626	$\bar{2}$	1	2	6	1.787	$\bar{3}$	4	2
9	2.514	$\bar{3}$	2	1			0	3	3
8	2.442	1	4	1	7	1.776	$\bar{3}$	5	1
		$\bar{2}$	2	2	16	1.750	2	6	0
25	2.411	3	1	1			$\bar{2}$	5	2
16	2.376	0	3	2	14	1.738	$\bar{2}$	3	3
9	2.311	3	3	0			5	0	0
8	2.300	$\bar{2}$	4	1			4	3	1
7	2.286	$\bar{3}$	0	2			3	3	2
7	2.271	2	1	2	16	1.727	$\bar{5}$	1	1
		3	2	1			$\bar{4}$	4	1
8	2.259	$\bar{3}$	3	1	14	1.720	5	1	0
7	2.222	1	5	0			$\bar{3}$	2	3
		1	3	2	14	1.710	2	1	3
7	2.149	0	5	1	9	1.681	3	5	1
		2	2	2	10	1.654	2	2	3
9	2.137	4	1	0			0	4	3
5	2.124	$\bar{3}$	2	2	5	1.631	2	5	2
12	2.059	1	5	1			4	1	2
9	2.040	3	4	0	15	1.613	1	7	0
9	2.033	4	2	0			4	4	1
		2	5	0	8	1.599	$\bar{4}$	1	3
15	1.971	$\bar{2}$	5	1			3	6	0

zones, which may suggest its metasomatic origin (Włodek *et al.*, 2015). At Michałkowa, another anatectic pegmatite of LCT type in the Góry Sowie gneissic block [type locality for graftonite-(Ca)], graftonite-(Mn) forms lamellar intergrowths with sarcopside and triphylite, and grades progressively to graftonite-(Ca). It is most likely a product of exsolution of Ca-enriched graftonite in the outer zones of phosphate nodules due to diffusion of Ca^{2+} within the hydrosaline melt towards the fluorapatite rim. Calcium-rich graftonite-(Ca) (Ca ~ 1 apfu), occurs only as single subhedral crystals close to the border of the primary magmatic phosphates of the unaltered interior of the nodule, with metasomatic phosphates closer to the nodule border, indicating the action of the high-T fluid released by the hydrosaline melt, which induced incipient Na- and Ca-metasomatism of the primary magmatic phosphates.

Both graftonite-(Mn) and graftonite-(Ca) are common pegmatite phosphates; they should be the main graftonite-group minerals in less-evolved phosphate-bearing pegmatites. In the last dozen years, the presence of graftonite with compositions corresponding to graftonite-(Mn) and graftonite-(Ca) has been well-documented, beside the above-

TABLE 9. Simulated powder pattern for graftonite-(Ca).

I	*d* (Å)	*h*	*k*	*l*
5	7.020	1	1	0
6	4.978	$\bar{1}$	1	1
14	4.387	1	1	1
7	4.298	0	2	1
10	3.733	$\bar{2}$	1	1
		1	2	1
100	3.654	1	3	0
6	3.266	$\bar{1}$	3	1
		2	1	1
56	3.133	$\bar{1}$	0	2
57	3.097	1	3	1
76	3.042	0	4	0
		$\bar{1}$	1	2
77	3.014	2	3	0
85	2.979	2	2	1
9	2.920	3	1	0
12	2.894	1	4	0
68	2.834	$\bar{3}$	1	1
13	2.784	1	1	2
7	2.758	$\bar{2}$	1	2
5	2.704	$\bar{1}$	4	1
7	2.649	$\bar{3}$	2	1
		2	3	1
5	2.610	1	4	1
		1	1	2
4	2.589	$\bar{2}$	2	2
30	2.542	3	1	1
		0	3	2
10	2.466	$\bar{2}$	4	1
		3	3	0
		2	0	2
8	2.418	2	1	2
		$\bar{3}$	3	1
10	2.389	$\bar{3}$	1	2
		1	3	2
6	2.311	2	2	2
		$\bar{1}$	5	1
9	2.288	$\bar{3}$	2	2
		4	1	0
12	2.254	1	5	1
12	2.226	2	5	0
		3	4	0
13	2.170	$\bar{2}$	5	1
		1	4	2
		0	1	3
15	2.147	$\bar{3}$	3	2
5	2.129	0	6	0
28	2.112	$\bar{2}$	1	3
		$\bar{1}$	2	3
11	2.095	$\bar{4}$	0	2
		3	1	2
		0	2	3
13	2.074	4	3	0
		$\bar{4}$	1	2
11	2.068	$\bar{4}$	3	1
		3	4	1
		1	1	3
15	2.046	0	6	1
		$\bar{2}$	2	3
8	2.006	$\bar{1}$	3	3
		1	2	3
9	1.993	1	6	1
		0	3	3
		$\bar{3}$	5	1
15	1.977	2	6	0
		1	5	2
15	1.970	$\bar{2}$	5	2
14	1.954	4	3	1
		3	3	2
		$\bar{4}$	4	1
		5	0	0
10	1.928	$\bar{5}$	1	1
		$\bar{3}$	2	3
		$\bar{4}$	3	2
16	1.920	5	1	0
		1	3	3
		2	1	3
10	1.907	3	5	1
8	1.881	$\bar{5}$	2	1
		0	4	3
11	1.876	5	2	0
		2	2	3
10	1.863	2	5	2
		1	7	0
		0	6	2
		4	0	2
		$\bar{1}$	6	2
8	1.843	4	4	1
		3	4	2
		3	6	0
8	1.829	$\bar{4}$	1	3
		$\bar{1}$	7	1
		1	4	3
7	1.798	$\bar{5}$	2	2
		2	7	0
12	1.782	5	2	1
		$\bar{1}$	5	3
		$\bar{1}$	0	4

mentioned Polish pegmatites, in Canadian, Swedish and Czech pegmatites described by Černý *et al.* (1998), Smeds *et al.* (1998) and Tait *et al.* (2013).

Acknowledgements

We thank Alessandro Guastoni and Peter Leverett, as well as Stuart Mills (Principal Editor) for their comments on this manuscript. The work was supported by the AGH UST grant 11.11.140.158 to AP, National Science Centre (Poland) grant 2015/17/N/ST10/02666 to AW, and by a Natural Sciences and Engineering Research Council of Canada Discovery grant, and by Canada Foundation for Innovation grants to FCH.

Supplementary material

To view supplementary material for this article, please visit https://doi.org/10.1180/minmag.2017.081.109.

References

Aftalion, M. and Bowes, D.R. (2002) U–Pb zircon isotopic evidence for Mid-Devonian migmatite formation in the Góry Sowie domain of the Bohemian Massif, Sudeten Mountains, SW Poland. *Neues Jahrbuch für Mineralogie, Monatshefte*, **4**, 182–192.

Bild, R.W. (1974) New occurrences of phosphates in iron meteorites. *Contributions to Mineralogy and Petrology*, **45**, 91–98.

Bröcker, M., Żelaźniewicz, A. and Enders, M. (1998) Rb–Sr and U–Pb geochronology of migmatitic gneisses from the Góry Sowie (West Sudetes, Poland): the importance of Mid–Late Devonian metamorphism. *Journal of the Geological Society, London*, **155**, 1025–1036.

Brooks, J.H. and Shipway, C.H. (1960) Mica Creek pegmatites, Mount Isa, North-western Queensland. *Australian Queensland Goverment Mining Journal*, **61**, 511–522.

Brueckner, H.K., Blusztajn, J. and Bakun-Czubarow, N. (1996) Trace element and Sm–Nd "age" zoning in garnets from peridotites of the Caledonian and Variscan mountains and tectonic implications. *Journal of Metamorphic Geology*, **14**, 61–73.

Calvo, C. (1968) The crystal structure of graftonite. *American Mineralogist*, **53**, 742–750.

Černý, P. and Ercit, T.S. (2005) The classification of granitic pegmatites revisited. *Canadian Mineralogist*, **43**, 2005–2026.

Černy, P., Selway, J.B., Ercit, T.S., Breaks, F.W., Anderson, A.J. and Anderson, S.D. (1998) Graftonite-beusite in granitic pegmatites of the Superior Province: A study in contrasts. *Canadian Mineralogist*, **36**, 367–376.

Chen, M. and Xie, X. (1996) Na behaviour in shock-induced melt phase of the Yanzhuang (H6) chondrite. *European Journal of Mineralogy*, **8**, 325–333.

Floss, C. (1999) Fe,Mg,Mn-bearing phosphates in the GRA 95209 meteorite: Occurrences and mineral chemistry. *American Mineralogist*, **84**, 1354–1359.

Fransolet, A.M. (1977) Intercroissances et inclusions dans les associations graftonite-sarcopside-triphylite. *Bulletin de la Societé Française de Minéralogie et de Cristallographie*, **100**, 198–207.

Gaines, R.V., Skinner, H.C.W., Foord, E.E., Mason, B. and Rosenwieg, A. (1997) *Dana's New Mineralogy*, Eighth Edition. Wiley and Sons, New York.

Gordon, S.M., Schneider, D.A., Manecki, M. and Holm, D.K. (2005) Exhumation and metamorphism of an ultrahigh-grade terrane: geochronometric investigations of the Sudetes Mountains (Bohemia), Poland and Czech Republic. *Journal of the Geological Society, London*, **162**, 841–855.

Grochowina, A. (2016) *Mineralogical studies of the Michałkowa pegmatite*. Doctorate thesis, AGH University of Science and Technology, Cracow, Poland [in Polish].

Guastoni, A., Nestola, F., Mazzoleni, G. and Vignola, P. (2007) Mn-rich graftonite, ferrisicklerite, staněkite and Mn-rich vivianite in a granitic pegmatite at Soè Valley, central Alps, Italy. *Mineralogical Magazine*, **71**, 579–585.

Hawthorne, F.C. and Pieczka, A. (2018) Classification of the minerals of the graftonite group. *Mineralogical Magazine*, **82**, 1301–1306.

Hawthorne, F.C., Ungaretti, L. and Oberti, R. (1995) Site populations in minerals: terminology and presentation of results of crystal-structure refinement. *Canadian Mineralogist*, **33**, 907–911.

Hawthorne, F.C., Wise, M.A., Černý, P., Abdu, Y.A., Ball, N., Pieczka, A. and Włodek, A. (2018) Beusite-(Ca), ideally $\mathrm{CaMn_2^{2+}(PO_4)_2}$, a new graftonite-group mineral from the Yellowknife pegmatite field, Northwest Territories, Canada: description and crystal structure. *Mineralogical Magazine*, **82**, 1323–1332.

Keller, P., Fontan, F., Velasco Roldan, F., Melgarejo, J.C. and Draper, I. (1977) Staněkite, a new phosphate mineral in pegmatites at Karibib (Namibia) and French Pyrénées (France). *European Journal of Mineralogy*, **9**, 475–482.

Kryza, R. (1981) Migmatization in gneisses of the northern part of the Sowie Góry, Sudetes. *Geologia Sudetica*, **16**, 7–91 [in Polish, English summary].

Kryza, R. and Fanning, C.M. (2007) Devonian deep-crustal metamorphism and exhumation in the Variscan Orogen: evidence from SHRIMP zircon ages from the HT–HP granulites and migmatites of the Góry

Sowie (Polish Sudetes). *Geodinamica Acta*, **20**, 159–176.

Łodziński, M. and Sitarz, M. (2009) Chemical and spectroscopic characterization of some phosphate accessory minerals from pegmatites of the Sowie Gory Mts., SW Poland. *Journal of Molecular Structure*, **924**, 442–447.

Mazur, S., Aleksandrowski, P., Kryza, R. and Oberc-Dziedzic, T. (2006) The Variscan Orogen in Poland. *Geological Quarterly*, **50**, 89–118.

Novák, M. (2005) Granitic pegmatites of the Bohemian Massif (Czech Republic); mineralogical, geochemical and regional classification and geological significance. *Acta Museum Moraviae, Scientiae Geologicae*, **90**, 3–75 [in Czech, English summary].

O'Brien, P.J., Kröner, A., Jaeckel, P., Hegner, E., Żelaźniewicz, A. and Kryza, R. (1997) Petrological and isotope studies on Palaeozoic high-pressure granulites. Góry Sowie Mts, Polish Sudetes. *Journal of Petrology*, **38**, 433–456.

Olsen, E. and Fredriksson, K. (1966) Phosphates in iron and pallasite meteorites: *Geochimica et Cosmochimica Acta*, **30**, 459–470.

Olsen, E.J., Kracher, A., Davis, A.M., Steele, I.M., Hutcheon, I.D. and Bunch, T.E. (1999) The phosphates of IIIAB iron meteorites. *Meteoritics & Planetary Science*, **34**, 285–300.

Penfield, S.L. (1900) On graftonite, a new mineral from Grafton, New Hampshire and its intergrowth with triphylite. *American Journal of Science*, **159**, 20–32.

Pieczka, A., Gołębiowska, B. and Skowroński, A. (2003) Ferrisicklerite and other phosphate minerals from the Lutomia pegmatite (SW Poland, Lover Silesia, Góry Sowie Mts). *International Symposium on Light Elements in Rock-forming Minerals.* Nové Město na Moravě, Czech Republic, June 20 to 25. Book of abstracts, pp. 63–64.

Pieczka, A., Szuszkiewicz, A., Szełęg, E., Nejbert, K., Łodziński, M., Ilnicki, S., Turniak, K., Banach, M., Hołub, W., Michałowski, P. and Różniak, R. (2013) (Fe,Mn)–(Ti,Sn)–(Nb,Ta) oxide assemblage in a little fractionated portion of a mixed (NYF + LCT) pegmatite from Piława Górna, the Sowie Mts. block, SW Poland. *Journal of Geosciences*, **58**, 91–112.

Pieczka, A., Szuszkiewicz, A., Szełęg, E., Ilnicki, S., Nejbert, K. and Turniak, K. (2014) Samarskite-group minerals and alteration products: an example from the Julianna pegmatitic system, Piława Górna, SW Poland. *Canadian Mineralogist*, **52**, 303–319.

Pieczka, A., Hawthorne, F.C., Cooper, M.A., Szełęg, E., Szuszkiewicz, A., Turniak, K., Nejbert, K. and Ilnicki, S. (2015*a*) Pilawite-(Y), $Ca_2(Y,Yb)_2[Al_4(SiO_4)4O_2(OH)_2]$, a new mineral from the Piława Górna granitic pegmatite, southwestern Poland: mineralogical data, crystal structure and association. *Mineralogical Magazine*, **79**, 1143–1157.

Pieczka, A., Szuszkiewicz, A., Szełęg, E., Janeczek, J. and Nejbert, K. (2015*b*): Granitic pegmatites of the Polish part of the Sudetes (NE Bohemian massif, SW Poland). *7th International Symposium on Granitic Pegmatites.* Książ, Poland, June 17–19, 2015. Fieldtrip Guidebook, C 73–103.

Pieczka, A., Włodek, A., Gołębiowska, B., Szełęg, E., Szuszkiewicz, A., Ilnicki, S., Nejbert, K. and Turniak, K. (2015*c*) Phosphate-bearing pegmatites in the Góry Sowie Block and adjacent areas, Sudetes, SW Poland. *7th International Symposium on Granitic Pegmatites, PEG 2015.* Książ, Poland. Book of Abstracts, pp. 77–78.

Pieczka, A., Szełęg, E., Szuszkiewicz, A., Gołębiowska, B., Zelek, S., Ilnicki, S., Nejbert, K. and Turniak, K. (2016) Cs-bearing beryl evolving to pezzottaite from the Julianna pegmatitic system, SW Poland. *Canadian Mineralogist*, **54**, 115–124.

Pieczka, A., Hawthorne, F.C., Gołębiowska, B., Włodek, A. and Grochowina, A. (2017*a*) Maneckiite, ideally $NaCa_2Fe^{2+}_2(Fe^{3+}Mg)Mn_2(PO_4)_6(H_2O)_2$, a new phosphate mineral of the wicksite supergroup from the Michałkowa pegmatite, Góry Sowie block, southwestern Poland. *Mineralogical Magazine*, **81**, 723–736.

Pieczka, A., Hawthorne, F.C., Ma, C., Rossman, G.R., Szełęg, E., Szuszkiewicz, A., Turniak, K., Nejbert, K., Ilnicki, S.S., Buffat, P. and Rutkowski, B. (2017*b*) Żabińskiite, ideally $Ca(Al_{0.5}Ta_{0.5})(SiO_4)O$, a new mineral of the titanite group from the Piława Górna pegmatite, the Góry Sowie Block, southwestern Poland. *Mineralogical Magazine*, **81**, 591–610.

Pouchou, J.L. and Pichoir, F. (1985) "PAP" (phi-rho-z) procedure for improved quantitative microanalysis. Pp. 104–106 in: *Microbeam Analysis*, (J.T. Armstrong, editor). San Francisco Press, San Francisco.

Sharygin, V.V., Karmanov, N.S. and Podgornykh, N.M. (2016) Fe-phosphate globules in impact metal-troilite associations of Chelyabinsk meteorite. *79th Annual Meeting of the Meteoritical Society. Meteoritics & Planetary Science*, **51**, S1, https://doi.org/10.1111/maps.12698

Sheldrick, G.M. (2008) A short history of SHELX. *Acta Crystallographica*, **A64**, 112–122.

Simmons, W.B. and Webber, K.L. (2008) Pegmatite genesis: state of the art. *European Journal of Mineralogy*, **20**, 421–438.

Škoda, R., Staněk, J. and Čopjaková, R. (2007) Mineral associations of phosphate nodules from a granitic pegmatite at Cyrilov near Velké Meziříčí, Moldanubikum; Part 1: Primary and exsolved phases. *Acta Museum Moraviae, Scientiae Geologicae*, **92**, 59–74 [in Czech].

Smeds, S.A., Uher, P., Černý, P., Wise, M.A., Gustafsson, L. and Penner, P. (1998) Graftonite –

beusite in Sweden: primary phases, products of exsolution, and distribution in zoned populations of granitic pegmatites. *Canadian Mineralogist*, **36**, 377–394.

Smith, D.G.W. and Nickel, E.H. (2007) A system for codification for unnamed minerals: report of the Subcommittee for Unnamed Minerals of the IMA Commission on New Minerals, Nomenclature and Classification. *Canadian Mineralogist*, **45**, 983–1055.

Stalder, M. and Rozendaal, A. (2002) Graftonite in phosphatic iron formations associated with the mid-Proterozoic Gamsberg Zn-Pb deposit, Namaqua Province, South Africa. *Mineralogical Magazine*, **66**, 915–927.

Steele, I.M., Olsen, E., Pluth, J. and Davis, A.M. (1991) Occurrence and crystal structure of Ca-free beusite in the El Sampal IIIA iron meteorite. *American Mineralogist*, **76**, 1985–1989.

Strunz, H. and Nickel, E.H. (2001) *Strunz Mineralogical Tables, Ninth Edition*. Schweizerbart'sche Verlagsbuchhandlung, Stuttgart.

Szełęg, E., Zuzens, B., Hawthorne, F.C., Pieczka, A., Szuszkiewicz, A., Turniak, K., Nejbert, K., Ilnicki, S. S., Friis, H., Makovicky, E., Weller, M.T. and Lemée-Cailleau, M.-H. (2017) Bohseite, ideally $Ca_4Be_4Si_9O_{24}(OH)_4$, from the Piława Górna quarry, the Góry Sowie Block, SW Poland. *Mineralogical Magazine*, **81**, 35–46.

Szuszkiewicz, A., Szełęg, E., Pieczka, A., Ilnicki, S., Nejbert, K., Turniak, K., Banach, M., Łodziński, M., Różniak, R. and Michałowski, P. (2013) The Julianna pegmatite vein system at the Piława Górna mine, Góry Sowie Block, SW Poland – preliminary data on geology and descriptive mineralogy. *Geological Quarterly*, **57**, 467–484.

Szuszkiewicz, A., Pieczka, A., Szełęg, E., Turniak, K., Ilnicki, S. and Nejbert, K. (2016) The euxenite-group minerals and products of their alteration in the hybrid Julianna granitic pegmatite, Piława Górna, Sudetes, southwestern Poland. *Canadian Mineralogist*, **54**, 979–898.

Tait, K.T., Hawthorne, F.C. and Wise, M.A. (2013) The crystal structure of the graftonite-beusite minerals. *Canadian Mineralogist*, **51**, 653–662.

Timmermann, H., Parrish, R., Noble, S.R. and Kryza, R. (2000) New U-Pb monazite and zircon data from the Sudetes Mountains in SW Poland: evidence for a single-cycle Variscan orogeny. *Journal of the Geological Society, London*, **157**, 265–268.

Turniak, K., Pieczka, A., Kennedy, A.K., Szełęg, E., Ilnicki, S., Nejbert, K. and Szuszkiewicz, A. (2015) Crystallisation age of the Julianna pegmatite system (Góry Sowie Block, NE margin of the Bohemian massif): evidence from U-Th-Pb SHRIMP monazite and CHIME uraninite studies. *7th International Symposium on Granitic Pegmatites, PEG 2015*. Książ, Poland. Book of Abstracts, pp. 111–112.

van Breemen, O., Bowes, D.R., Aftalion, M. and Żelaźniewicz, A. (1988) Devonian tectonothermal activity in the Sowie Góry gneissic block, Sudetes, SW Poland: evidence from Rb-Sr and U-Pb isotopic studies. *Annales Socieatits Geologorum Poloniae*, **58**, 3–19.

Vignola, P., Diella, V., Oppizzi, P., Tiepolo, M. and Weiss, S. (2008) Phosphate assemblages from the Brissago granitic pegmatite, Western Southern Alps, Switzerland. *Canadian Mineralogist*, **46**, 635–650.

Vignola, P., Diella, V., Ferrari, E.S. and Fransolet, A.M. (2011*a*) Complex mechanisms of alteration in a graftonite + sarcopside + triphylite association from the Luna pegmatite, Piona, Lecco Province, Italy. *Canadian Mineralogist*, **49**, 765–776.

Vignola, P., Fransolet, A.M., Guastoni, A. and Appiani, R. (2011*b*) Le pegmatiti di Piona. Recenti studi sui filoni Malpensata, Luna e Sommafiume. *Rivista Mineralogica Italiana*, **35**, 30–38.

Websky, M. (1868) Über Sarkopsid und Kochelit, zwei neue Minerale aus Schlesien. *Zeitschrift der Deutschen Geologischen Gesellschaft*, **20**, 245–257.

Wise, M.A., Hawthorne, F.C. and Černý, P. (1990) Crystal structure of a Ca-rich beusite from the Yellowknife pegmatite field, North West Territories. *Canadian Mineralogist*, **28**, 141–146.

Włodek, A. and Pieczka, A. (2017) Mineral chemistry of the zigrasite–malhmoodite series from the granitic pegmatite at Lutomia (Góry Sowie block, SW Poland). *PEG2017, 8th International Symposium on Granitic Pegmatites, NGF.* Abstracts and Proceedings, **2**, 181–182.

Włodek, A., Grochowina, A., Gołębiowska, B. and Pieczka, A. (2015) A phosphate-bearing pegmatite from Lutomia and its relationships to other pegmatites of the Góry Sowie Block, southwestern Poland. *Journal of Geosciences*, **60**, 45–72.

Żelaźniewicz, A. (1990) Deformation and metamorphism in the Góry Sowie gneiss complex, Sudetes, SW Poland. *Neues Jahrbuch für Geologie und Paläontologie, Abhandlungen*, **179**, 129–157.